International Multidisciplinary Engineering Congress

Booklets

RENIECYT
Registro Nacional de Instituciones y Empresas Científicas y Tecnológicas
1702902 CONACYT

RENIECYT - LATINDEX - Research Gate - DULCINEA - CLASE - Sudoc - HISPANA - SHERPA UNIVERSIA - Google Scholar DOI - REDIB - Mendeley - DIALNET - ROAD - ORCID

Title: Noise analysis using Tucker Decomposition and PCA on spectral images

Author: PADILLA, Efraín, TORRES-ROMÁN, Deni Librado y MÉNDEZ-VÁZQUEZ, Andrés

Editorial label ECORFAN: 607-8695
BCONIMI Control Number: 2020-31
BCONIMI Classification (2020): 120320-0031

Pages: 32
RNA: 03-2010-032610115700-14

ECORFAN-México, S.C.
143 – 50 Itzopan Street
La Florida, Ecatepec Municipality
Mexico State, 55120 Zipcode
Phone: +52 1 55 6159 2296
Skype: ecorfan-mexico.s.c.
E-mail: contacto@ecorfan.org
Facebook: ECORFAN-México S. C.
Twitter: @EcorfanC

www.ecorfan.org

Holdings

Mexico, Colombia, Guatemala, Bolivia, Cameroon, Democratic Republic of Congo, Spain, El Salvador, Ecuador, Taiwan, Peru, Paraguay, Nicaragua

Content

1. Introduction
2. Problems
3. Noise assumptions
4. Compression
5. Phenomenology observed
6. Experiment
7. Conclusions
8. References

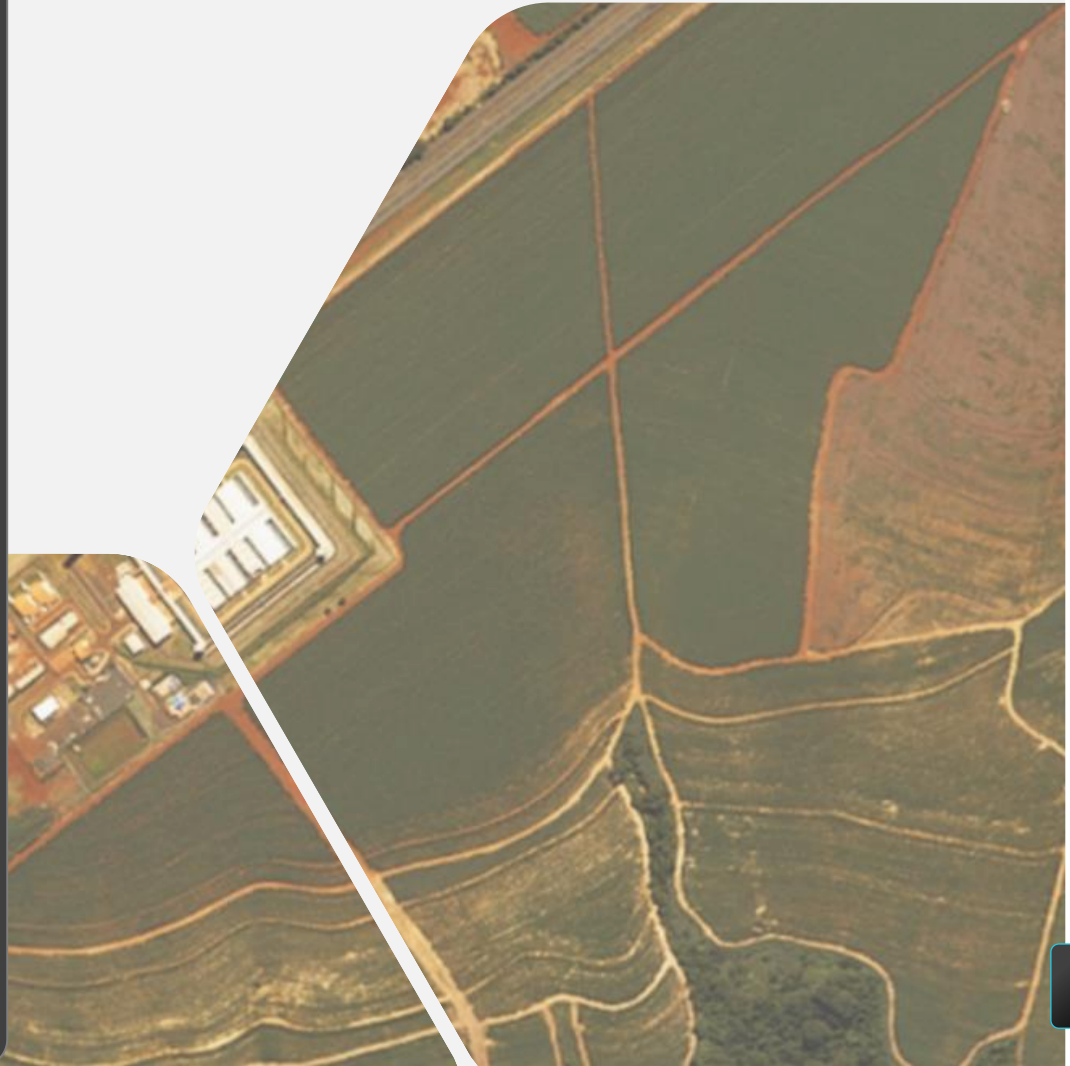

Introduction

Spectral Image (SI) definition:

- The greek word "**spectral**," which relates to "**colors**", combined with **image** figuratively mean "**Image of colors.**"
- Is based on taking a portion of the electromagnetic spectrum and **breaking it into pieces** for the purpose of **analytical computations**. [1]
- We represent the SI as a **tensor**.

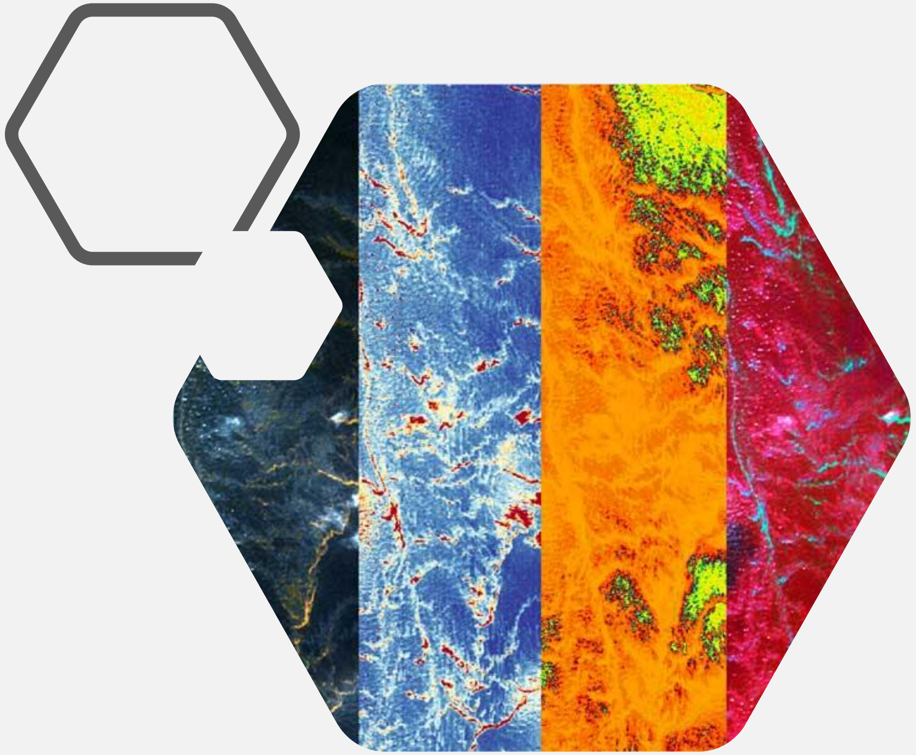

Fig.1 – HSI example

Tensor

- A tensor is a multidimensional array. The order of a tensor is the number of its dimensions, also called the ways or modes; therefore an Nth-order is an array with N dimensions. [2]

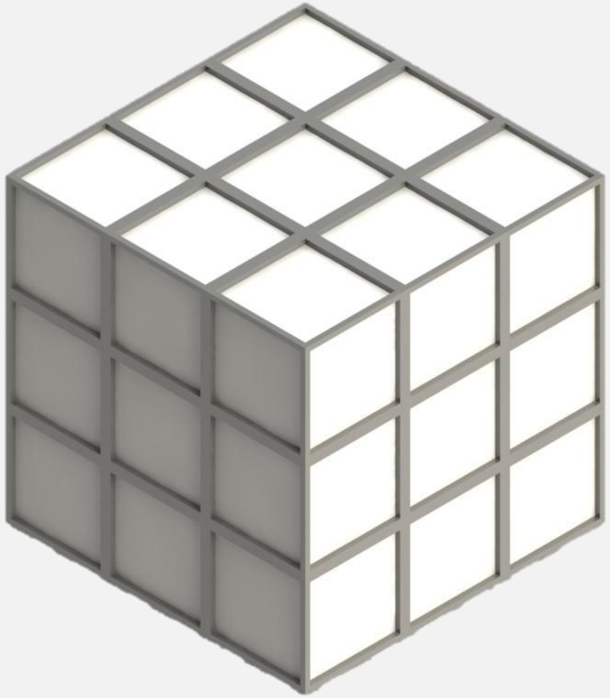

Fig.2 - Example of a 3rd-order tensor $\in \mathbb{R}^{3\times3\times3}$

Notation

x : a scalar.

$\mathbf{x}$: a 1st-order tensor or a vector.

$\mathbf{X}$: a 2nd-order tensor or a matrix.

$\mathcal{X}$: a 3rd or higher-order tensor.

$x_{i,j,\ldots,n}$: the element $(i, j, \ldots n)$ of a tensor $\mathcal{X}$.

$\mathbf{x}_i$: the ith column of a matrix $\mathbf{X}$.

Tensor Examples

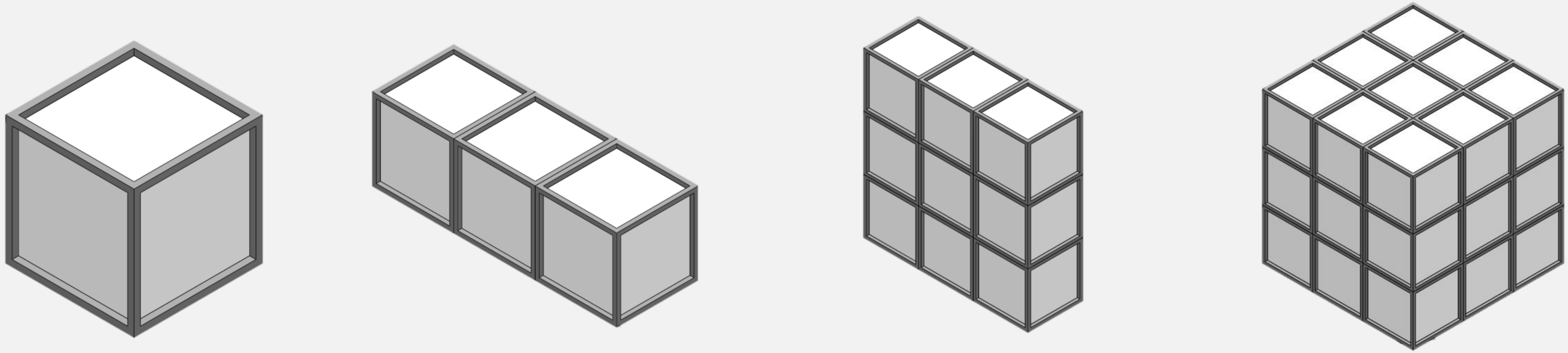

x : a scalar. | $\mathbf{x}$: a 1st-order tensor. | $\mathbf{X}$: a 2nd-order tensor. | $\mathcal{X}$: a 3rd-order tensor.

$x \in \mathbb{R}$ | $\mathbf{x} \in \mathbb{R}^3$ | $\mathbf{X} \in \mathbb{R}^{3\times3}$ | $\mathcal{X} \in \mathbb{R}^{3\times3\times3}$

Fig.3 – Tensor Examples

SI Representation

- We represent a SI as a 3rd-order tensor

$$\mathcal{H} : \text{Hyperspectral Image}$$

$$\mathcal{H} \in \mathbb{R}^{h \times w \times b}$$

$$h : \text{height}$$
$$w : \text{width}$$
$$b : \text{bands}$$

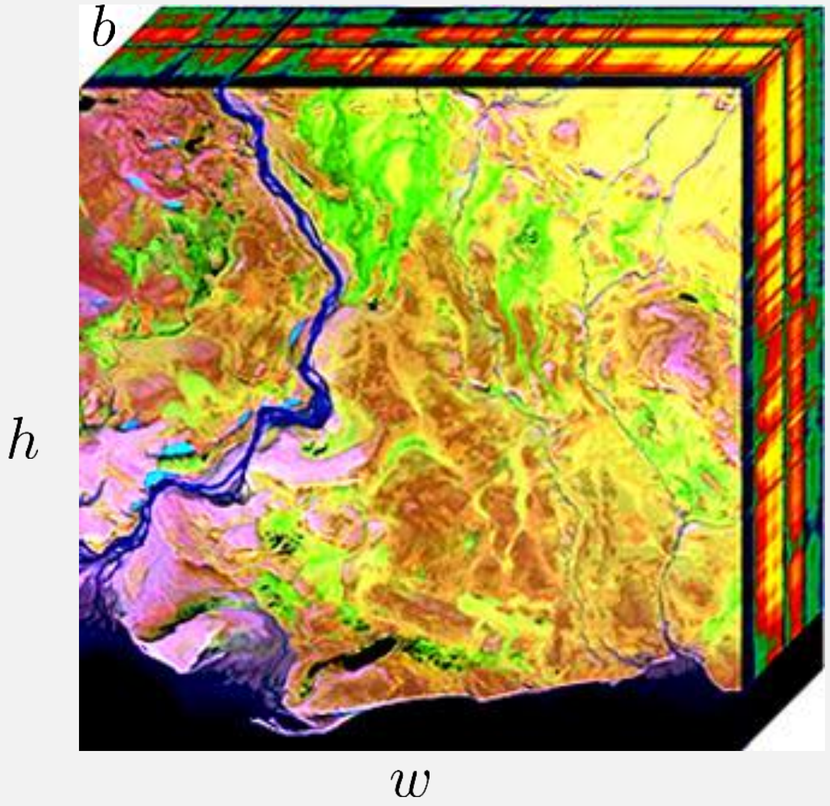

Fig.4 – SI

Where h, w and b are the number of pixels (elements) in
each Mode-1 (column), Mode-2 (row) and Mode-3 (tube) fibers respectively.

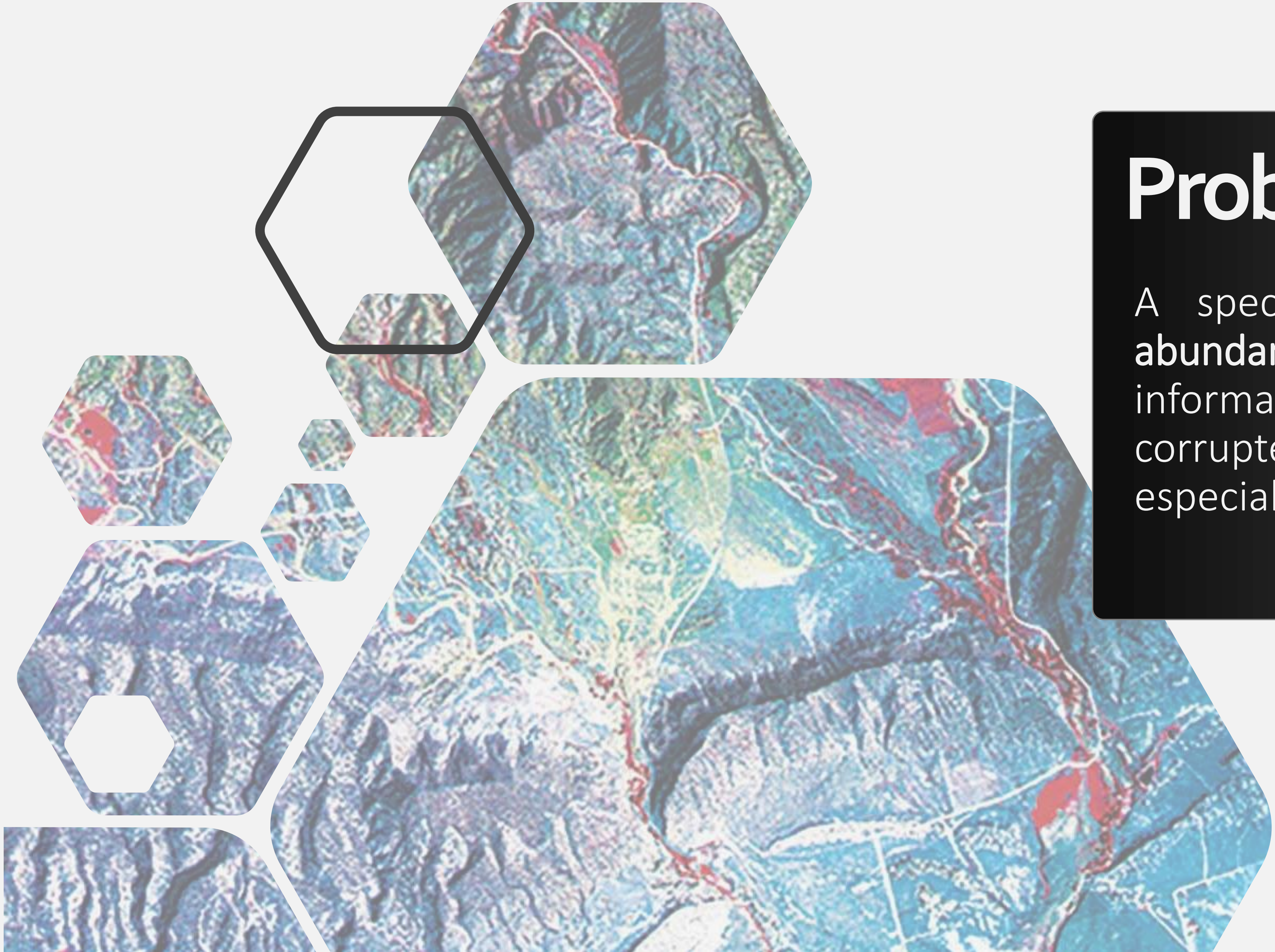

Problems

A spectral image contains **abundant** spatial and spectral information and is always corrupted by various **noises,** especially Gaussian noise. [3]

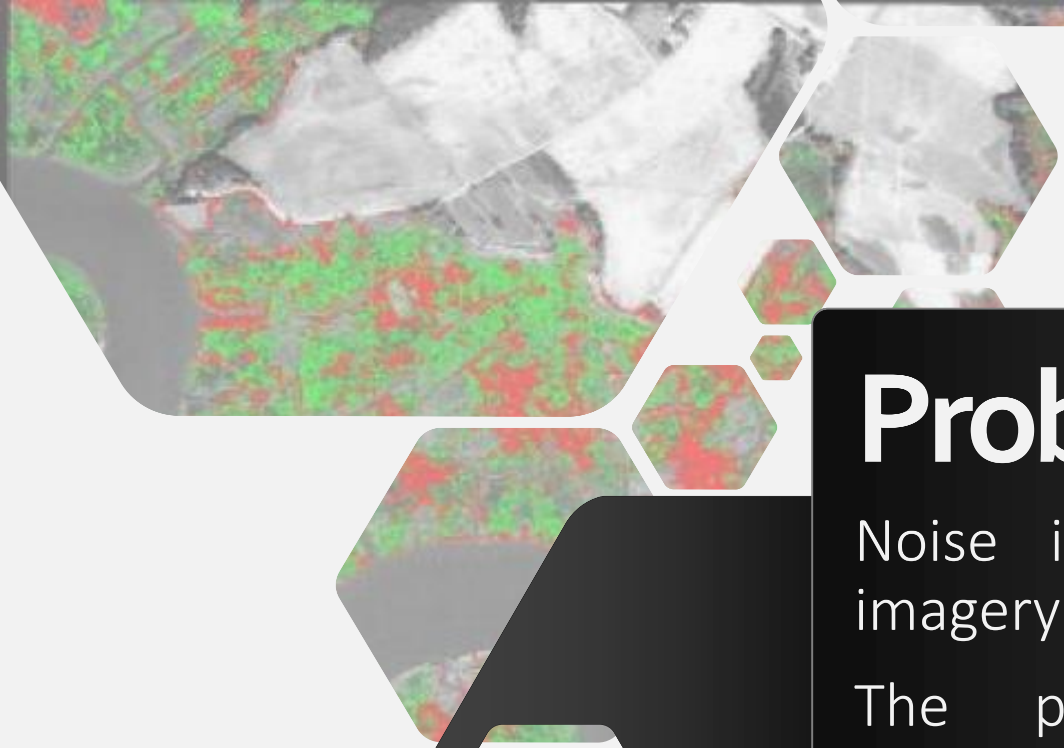

Problems

Noise is a problem in spectral imagery applications.

The performance of spectral analysis tasks (i.e. Classification) depends of the **SNR** of he spectral image. [4]

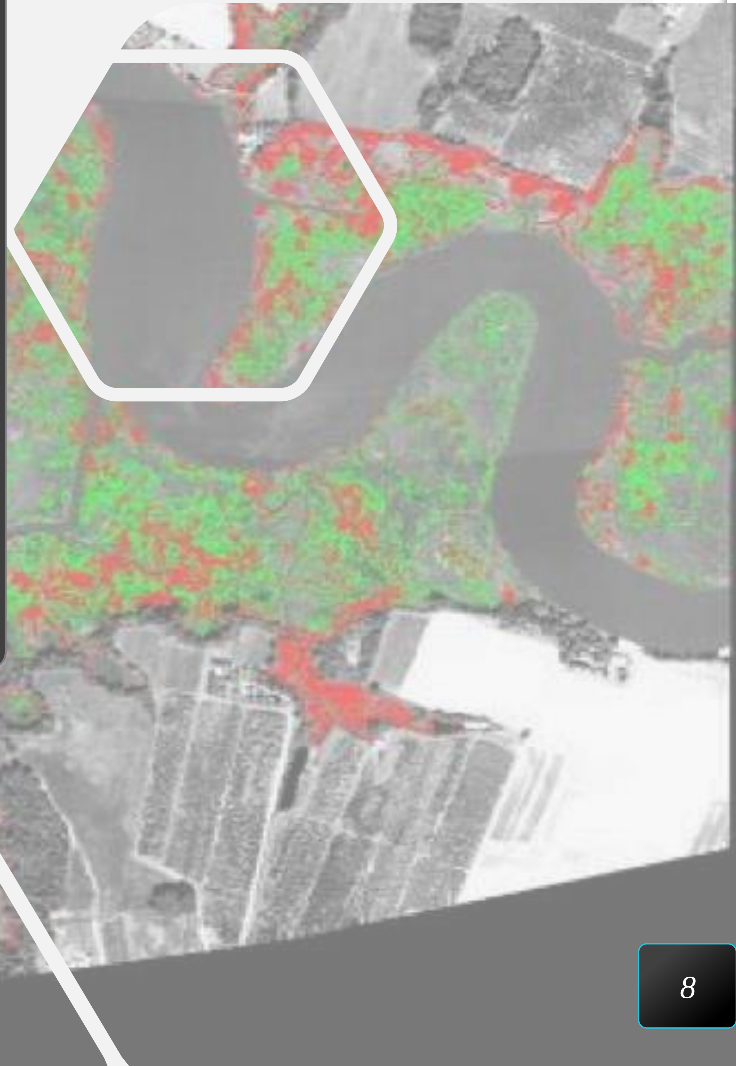

Before deal with the Noise…
We need to know about him.

Noise Assumptions [4]

- The presence of different noise sources in a SI makes its modeling and the denoising task very challenging
  - Therefore, SI denoising approaches often consider either of the following noise types or a mixture of them.

Noise Assumptions [4]

- Signal Independent Noise
  - Thermal noise and quantization noise in HSI are modeled by signal independent Gaussian additive noise. Usually, noise is assumed to be uncorrelated spectrally. The Gaussian assumption has been broadly used in hyperspectral analysis since it considerably simplifies the analysis and the noise variance estimation.
- Sparse Noise
  - Impulse noises such as salt and pepper noise, missing pixels, missing lines and other outliers often exist in the acquired HSI, and are usually due to a malfunctioning of the sensor.
- Pattern Noise
  - Hyperspectral imaging systems may also induce artifacts in hyperspectral images, usually referred to as pattern noise.

Additive Noise

- Generally, in the state of the art can be found many ways to get:

$$\mathcal{S} = \mathcal{X} + \mathcal{N}$$

- Where:

$$\mathcal{S}, \mathcal{X}, \mathcal{N} \in \mathbb{R}^{h \times w \times b}$$

$$\begin{aligned} &\mathcal{S} \rightarrow \text{Noisy SI} \\ &\mathcal{X} \rightarrow \text{Clean SI} \\ &\mathcal{N} \rightarrow \text{Noise} \end{aligned}$$

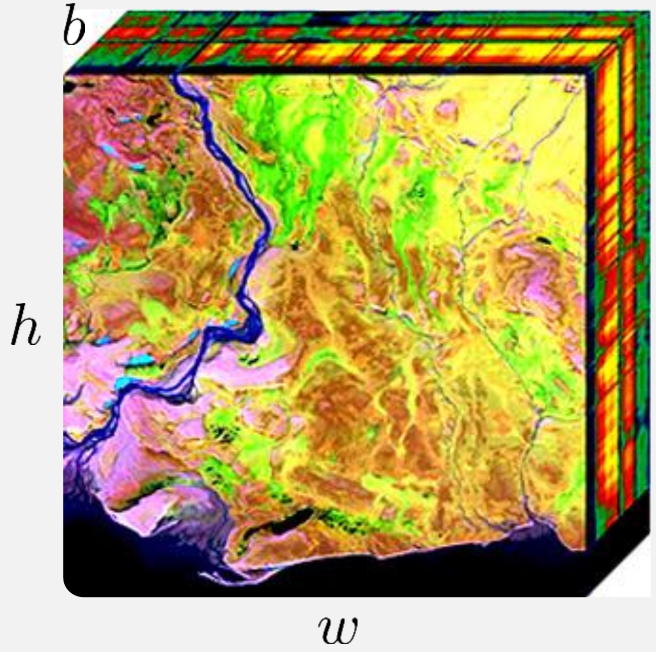

Fig.4 – SI

To deal with the size of the data…

Compression methods!

PCA

- Is a dimensionality reduction method, that is often used to reduce the dimensionality of large data sets, by transforming a large set of variables into smaller one that still contains most of the information in the large dataset.

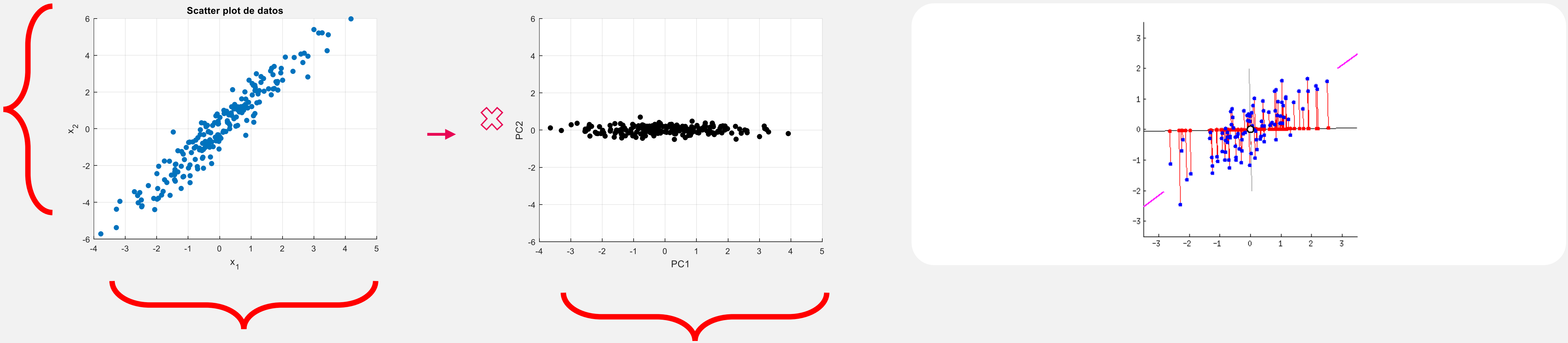

Fig.5 – PCA example

Tucker Tensor Decomposition

- Is a form of Higher Order of PCA. It decomposes a tensor into a core tensor multiplied (or transformed) by a matrix along each mode. Thus, in the three-way case where $\mathcal{X} \in \mathbb{R}^{I \times J \times K}$ we have. [2]
- To do compression only in the spectral domain we can make $\boldsymbol{A}, \boldsymbol{B} = \boldsymbol{I}$ (For semantic segmentation purposes)

$$\mathfrak{X} \approx \mathfrak{G} \times_1 \mathbf{A} \times_2 \mathbf{B} \times_3 \mathbf{C} = \sum_{p=1}^{P} \sum_{q=1}^{Q} \sum_{r=1}^{R} g_{pqr} \, \mathbf{a}_p \circ \mathbf{b}_q \circ \mathbf{c}_r = [\![\mathfrak{G} \, ; \mathbf{A}, \mathbf{B}, \mathbf{C}]\!].$$

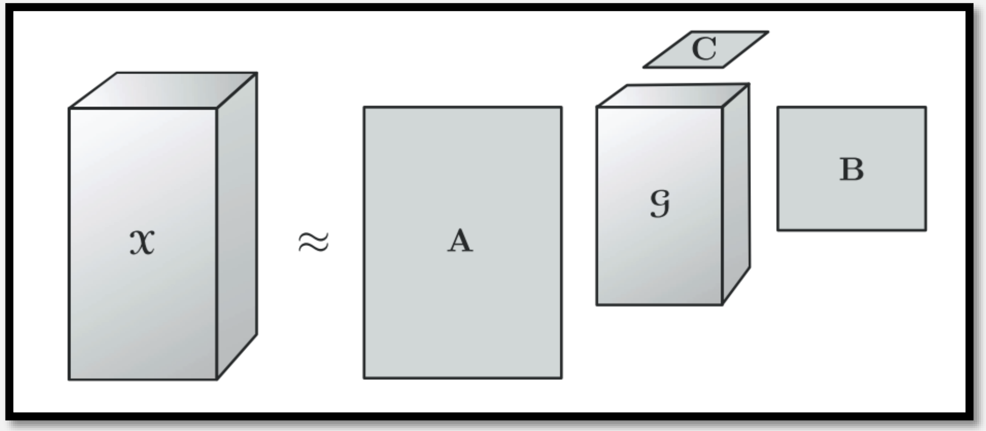

Fig.6 – Tucker Decomposition of a three way array

Phenomenology observed in [16]

Accuracy improvement after compression

Normally after a dataset compression stage we expect a loss of information and consequently a worse accuracy in classification tasks, but in this work the **accuracy improve** in some cases**!** **WHY?**

remote sensing

MDPI

Article

Spectral Imagery Tensor Decomposition for Semantic Segmentation of Remote Sensing Data through Fully Convolutional Networks

Josué López [1,*], Deni Torres [1], Stewart Santos [2] and Clement Atzberger [3]

1 Center for Research and Advanced Studies of the National Polytechnic Institute, Telecommunications Group, Av del Bosque 1145, Zapopan 45017, Mexico; dtorres@gdl.cinvestav.mx
2 University of Guadalajara, Center of Exact Sciences and Engineering, Blvd. Gral. Marcelino García Barragán 1421, Guadalajara 44430, Mexico; stewart.santos@academicos.udg.mx
3 University of Natural Resources and Life Science, Institute of Geomatics, Peter Jordan 82, Vienna 1180, Austria; clement.atzberger@boku.ac.at
* Correspondence: jalopez@gdl.cinvestav.mx

Received: 22 November 2019; Accepted: 11 January 2020; Published: 5 February 2020

check for updates

Abstract: This work aims at addressing two issues simultaneously: data compression at input space and semantic segmentation. Semantic segmentation of remotely sensed multi- or hyperspectral images through deep learning (DL) artificial neural networks (ANN) delivers as output the corresponding matrix of pixels classified elementwise, achieving competitive performance metrics. With technological progress, current remote sensing (RS) sensors have more spectral bands and higher spatial resolution than before, which means a greater number of pixels in the same area. Nevertheless, the more spectral bands and the greater number of pixels, the higher the computational complexity and the longer the processing times. Therefore, without dimensionality reduction, the classification task is challenging, particularly if large areas have to be processed. To solve this problem, our approach maps an RS-image or third-order tensor into a core tensor, representative of our input image, with the same spatial domain but with a lower number of new tensor bands using a Tucker decomposition (TKD). Then, a new input space with reduced dimensionality is built. To find the core tensor, the higher-order orthogonal iteration (HOOI) algorithm is used. A fully convolutional network (FCN) is employed afterwards to classify at the pixel domain, each core tensor. The whole framework, called here HOOI-FCN, achieves high performance metrics competitive with some RS-multispectral images (MSI) semantic segmentation state-of-the-art methods, while significantly reducing computational complexity, and thereby, processing time. We used a Sentinel-2 image data set from Central Europe as a case study, for which our framework outperformed other methods (included the FCN itself) with average pixel accuracy (PA) of 90% (computational time ~90s) and nine spectral bands, achieving a higher average PA of 91.97% (computational time ~36.5s), and average PA of 91.56% (computational time ~9.5s) for seven and five new tensor bands, respectively.

Keywords: fully convolutional network; semantic segmentation; spectral image; tensor decomposition

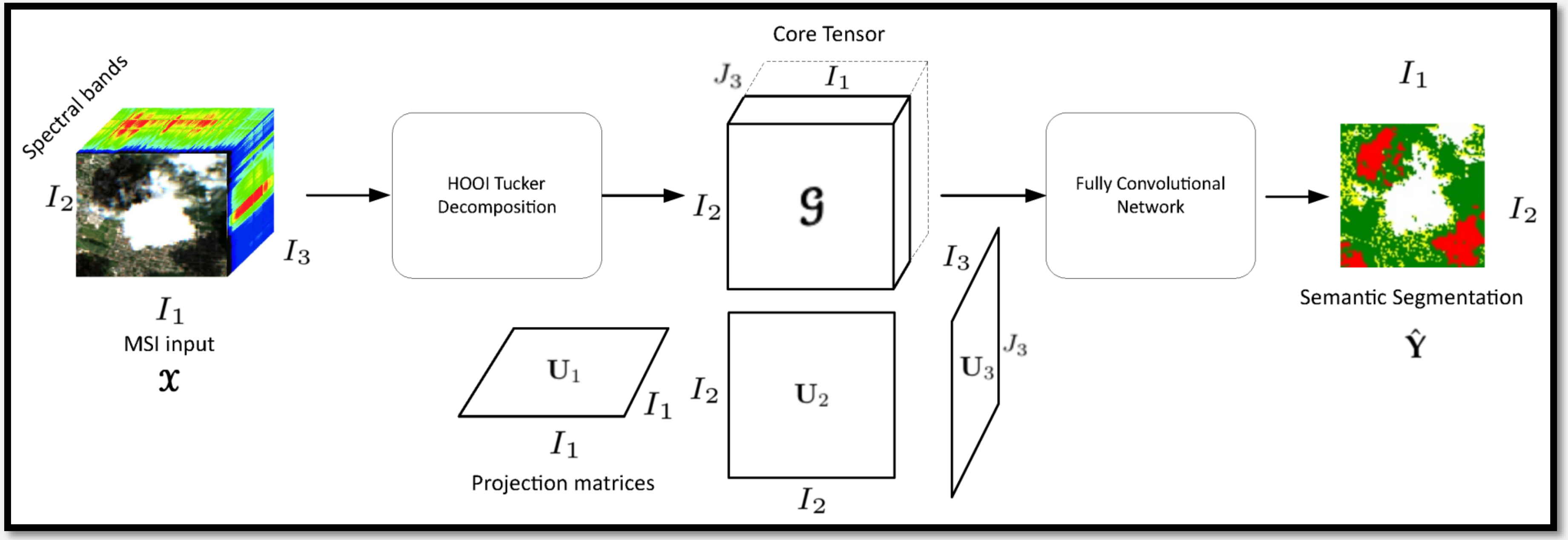

Fig.7 – Framework proposed in [16]

Experiment

Analyze the images and its classification accuracy through a Neural Network after PCA and Tucker compression

SI Dataset [16]

Real Dataset with simulated noise

- We used a Sentinel-2 image data set of 115 scenes of (128x128x9) from Central Europe (already with “natural” noise) with simulated additive noise as a case study, can be generated by zero-mean Gaussian noise as seen in [4]

$$\mathbf{N} = [n_{ij}] \text{ where } n_{ij} \sim N(0, \sigma_i^2) \text{ is normally distributed}$$

- The variance of the noise σ_i^2 variates along the spectral axis according to

$$\sigma_i^2 = \sigma^2 \frac{e^{-\frac{(i-p/2)^2}{2\eta^2}}}{\sum_{j=1}^{p} e^{-\frac{(j-p/2)^2}{2\eta^2}}}$$

Where the power of the noise is controlled by σ, and η behaves like the standard deviation of a Gaussian bell curve. p is the number of bands which is 9.

First Look

With $\sigma = 13$ and $\eta = 72$, $\text{scene} = 50$, $\text{band} = 1$

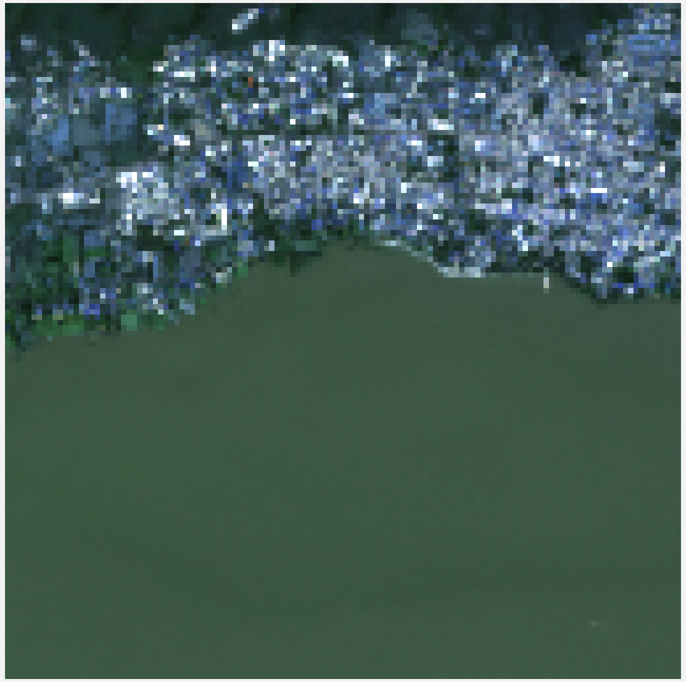

RGB Reference Image

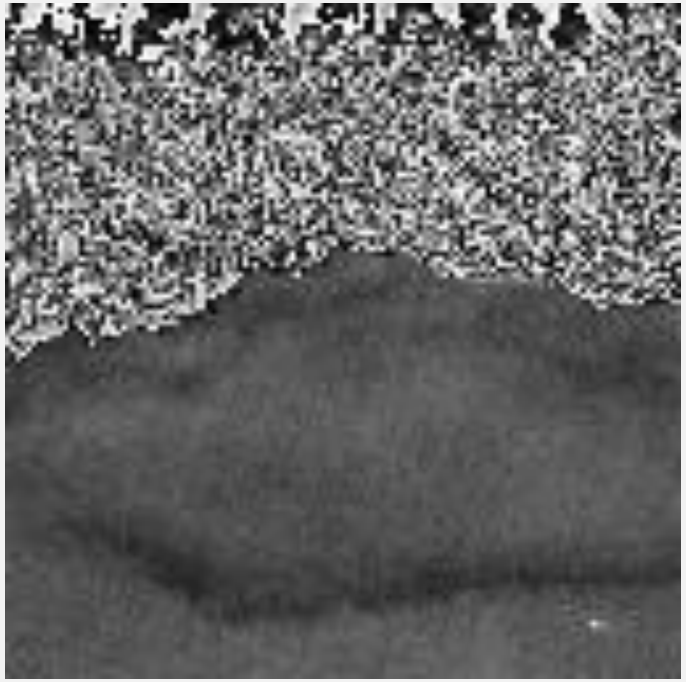

Band 1 – Original

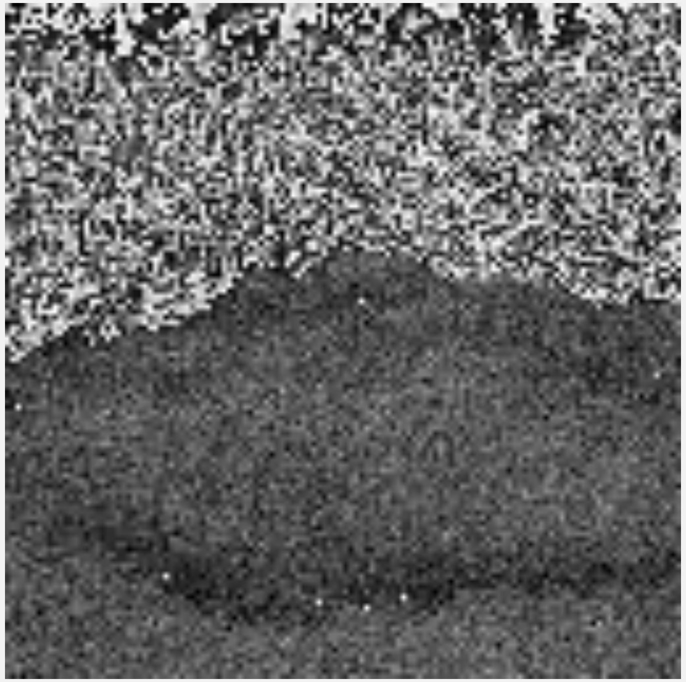

Band 1 – Noise added

Fig.7 –Noise adding to scene 50 – Visualization of band 1

First Look

With $\sigma = 13$ and $\eta = 72$, $\mathrm{scene} = 50$, $\mathrm{band} = 1$

$Compressed\ to\ 3\ components\ (PCA)/tensorial\ bands\ (Tucker)$

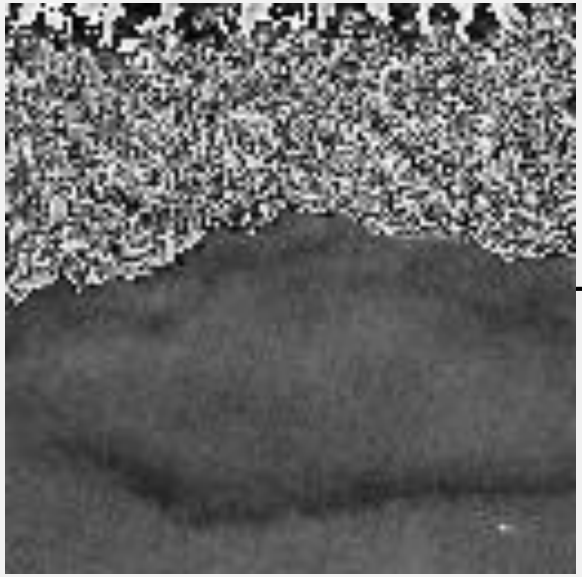

Band 1 – Original

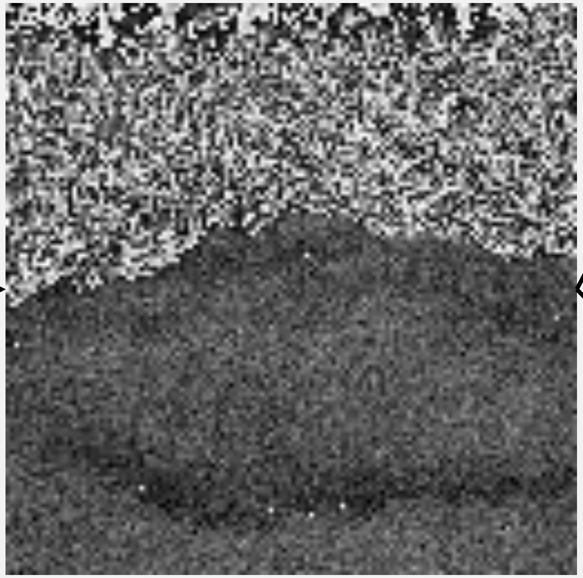

Band 1 – Noise added

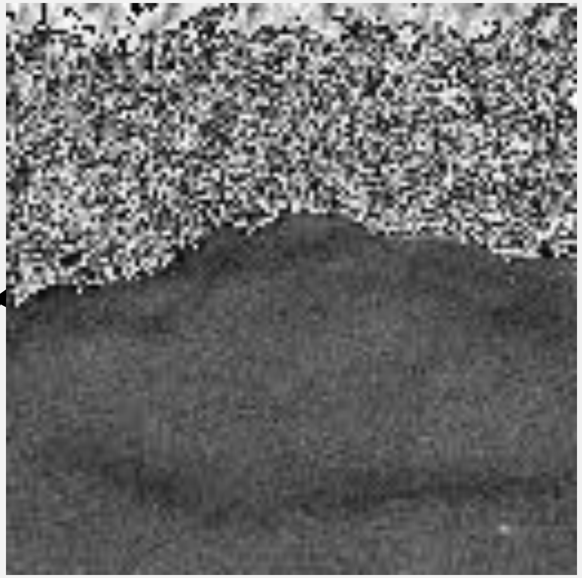

After PCA

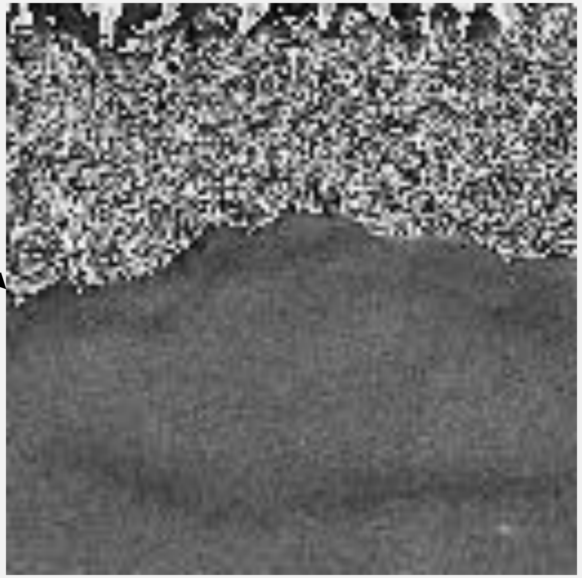

After Tucker Decomposition

Fig.8 –Visualization of compressed images of a noisy band

Noise parameters [17]

Real Dataset with simulated noise

- We set an average SNR (Signal to Noise Ratio) of 17dB. We get this with $\sigma = 82,\ SNR_{ave} = 17dB$

$$SNR = 10\log_{10}\frac{E(\mathbf{X}^T\mathbf{X})}{E(\mathbf{N}^T\mathbf{N})}$$

- The experiment were performed with different values of $\eta = 18, 36, 72$

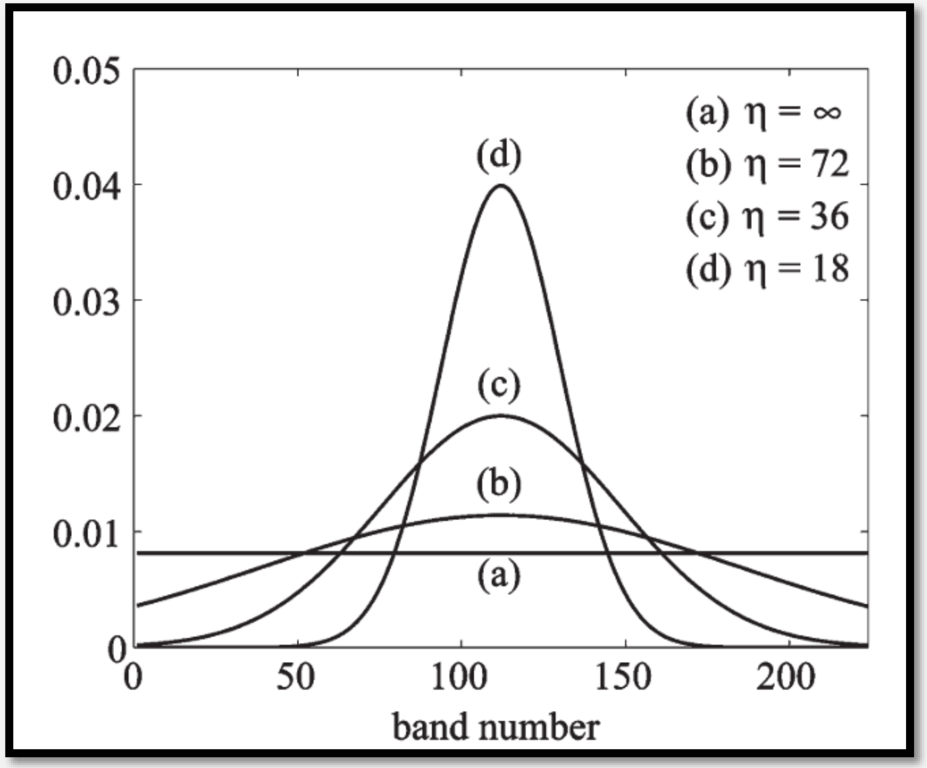

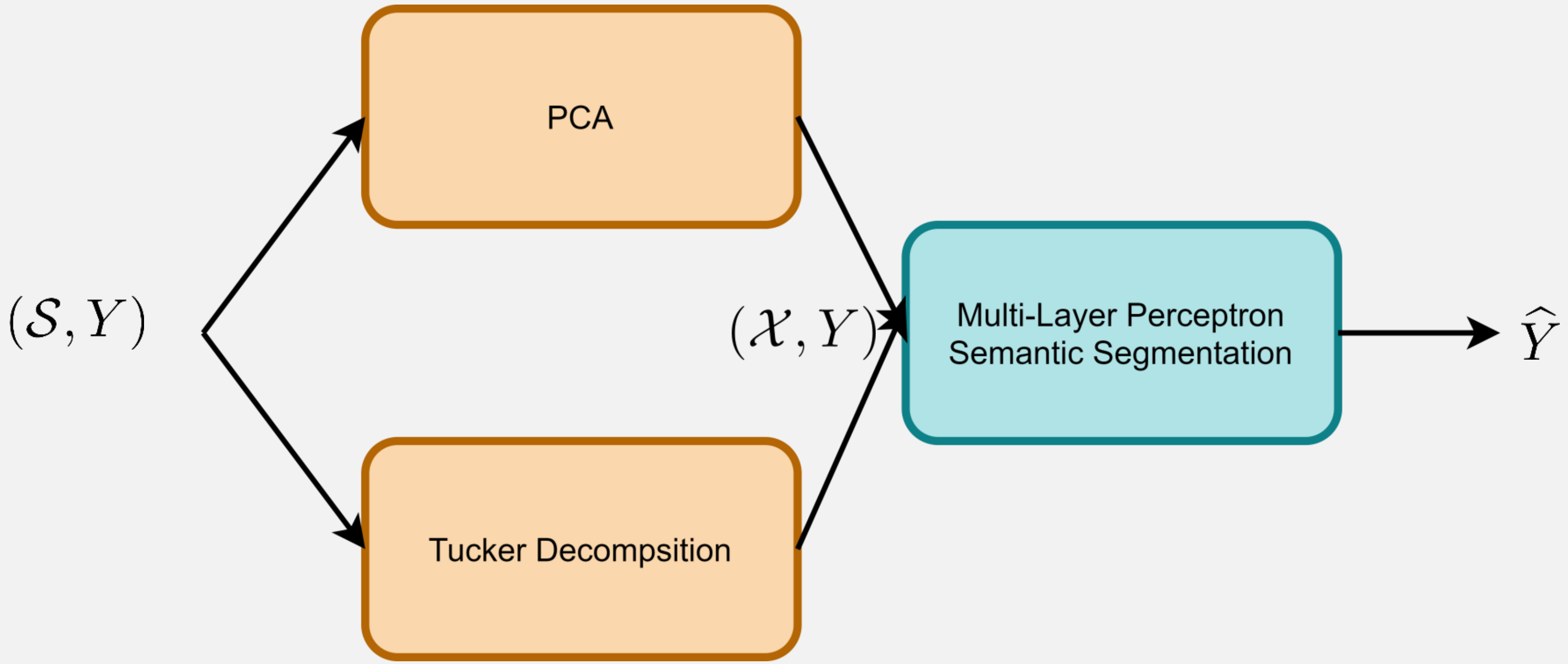

Fig.9 – Experiment workflow

Experiment

$\mathcal{S} \rightarrow$ Input noisy SI
$\mathcal{X} \rightarrow$ Clean SI
$Y \rightarrow$ Pixel labels
$\widehat{Y} \rightarrow$ Estimated pixel labels

$\mathcal{S}, \mathcal{X} \in \mathbb{R}^{w \times h \times b}$
$Y, \widehat{Y} \in \mathbb{R}^{w \times h}$

Multi-Layer Perceptron [18]

Artificial Neural Network as Classifier

- Parameters:
  - Hidden Layers: 2, Neurons per layer: 100
  - Activation function: ReLu
  - Solver for weight optimization: ADAM
  - Regularization term: L2 penalty
  - Batch size: 200
  - Learning rate: Adaptative
  - Iterations: 10
  - Train 70%/Test 30% picked random

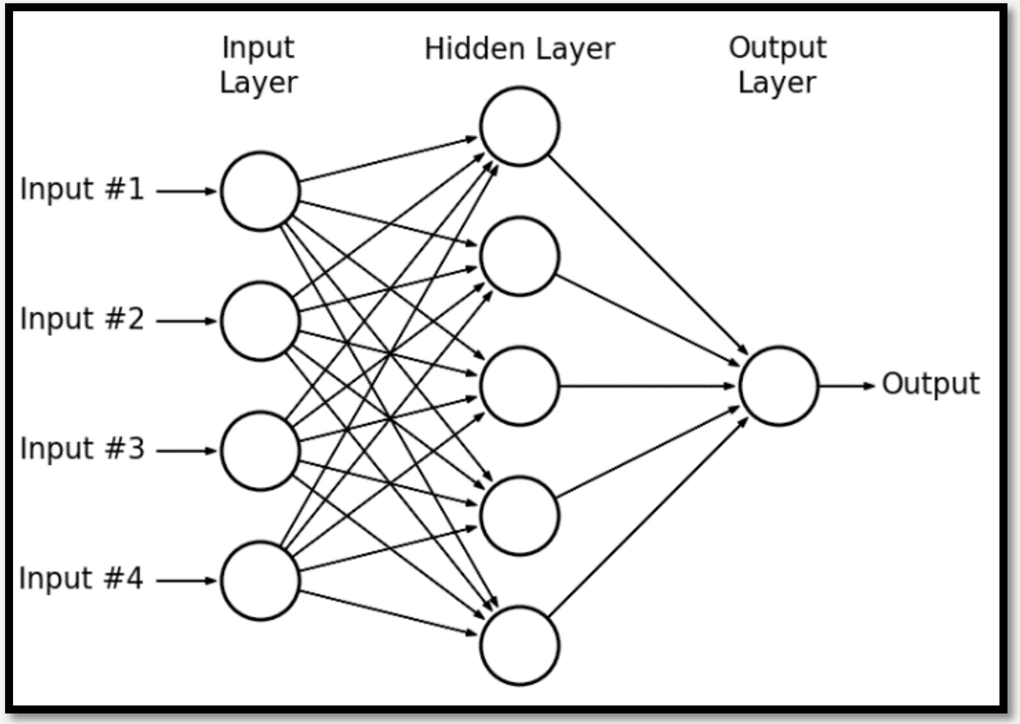

Fig.9 – MLP Example

- Data dimensions (vectorized) = (1,884,160 x PrincipalComponents) [PCA]
  = (1,884,160 x TensorialBands) [Tucker]

Accuracy Analysis – No Noise Added

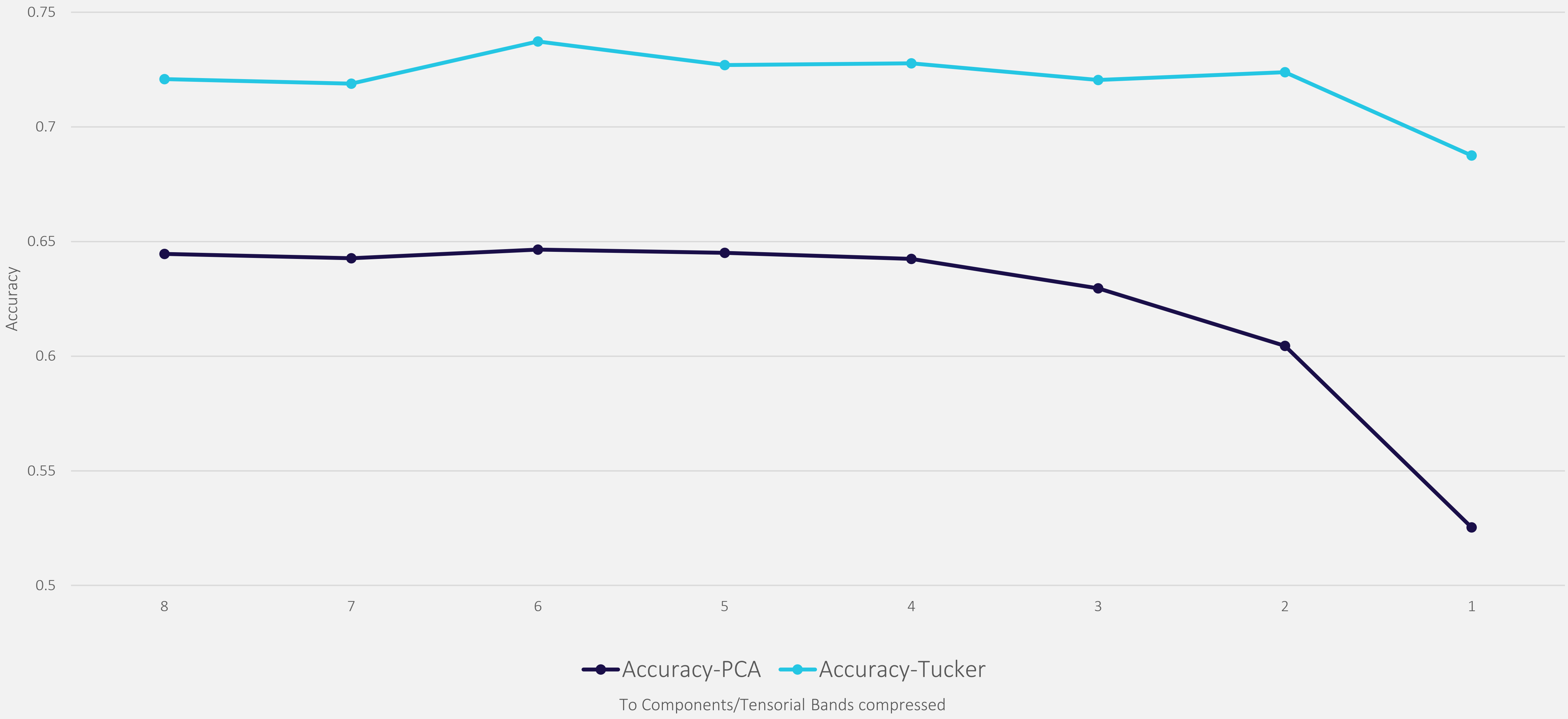

Accuracy Analysis – Noise Added: $\sigma = 82$ and $\eta = 16$

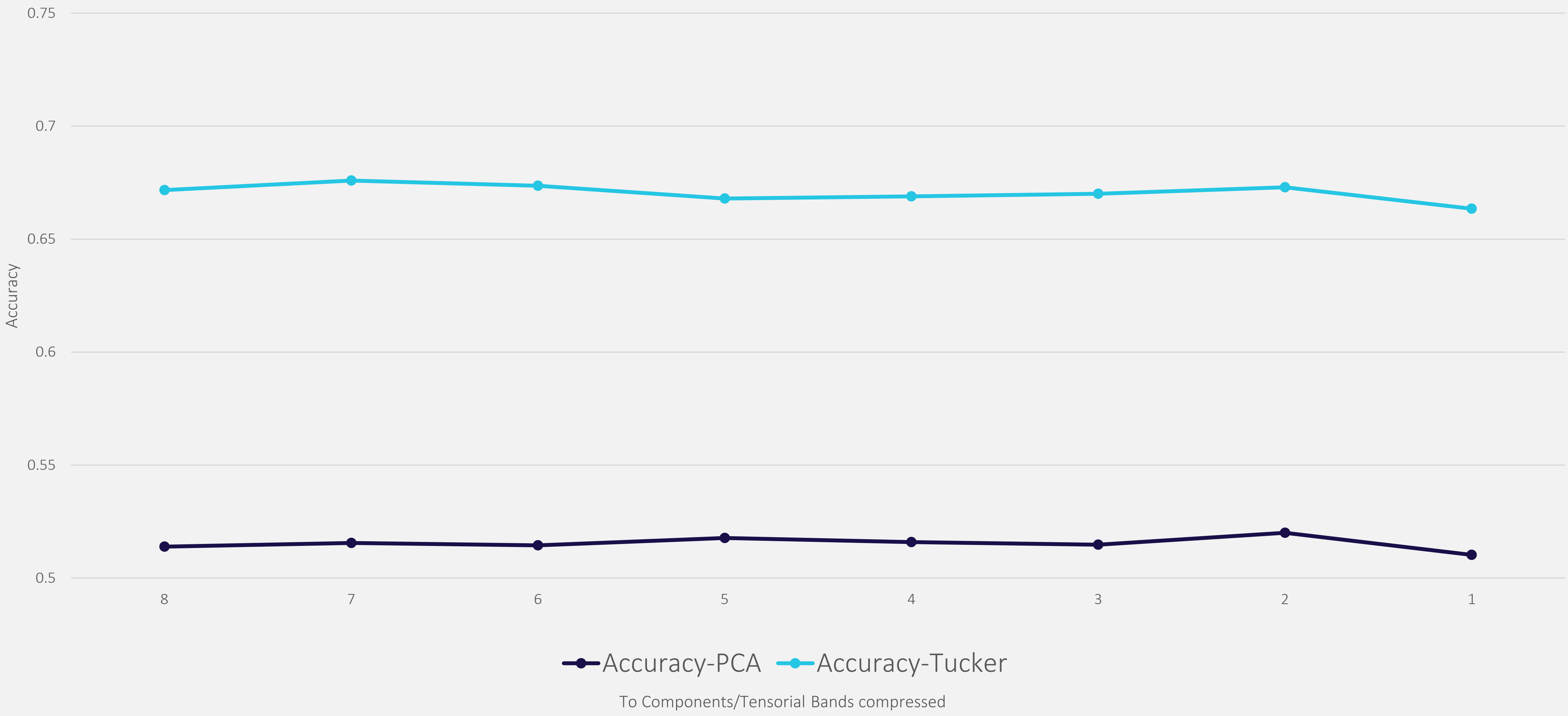

Accuracy Analysis – Noise Added: $\sigma = 82$ and $\eta = 36$

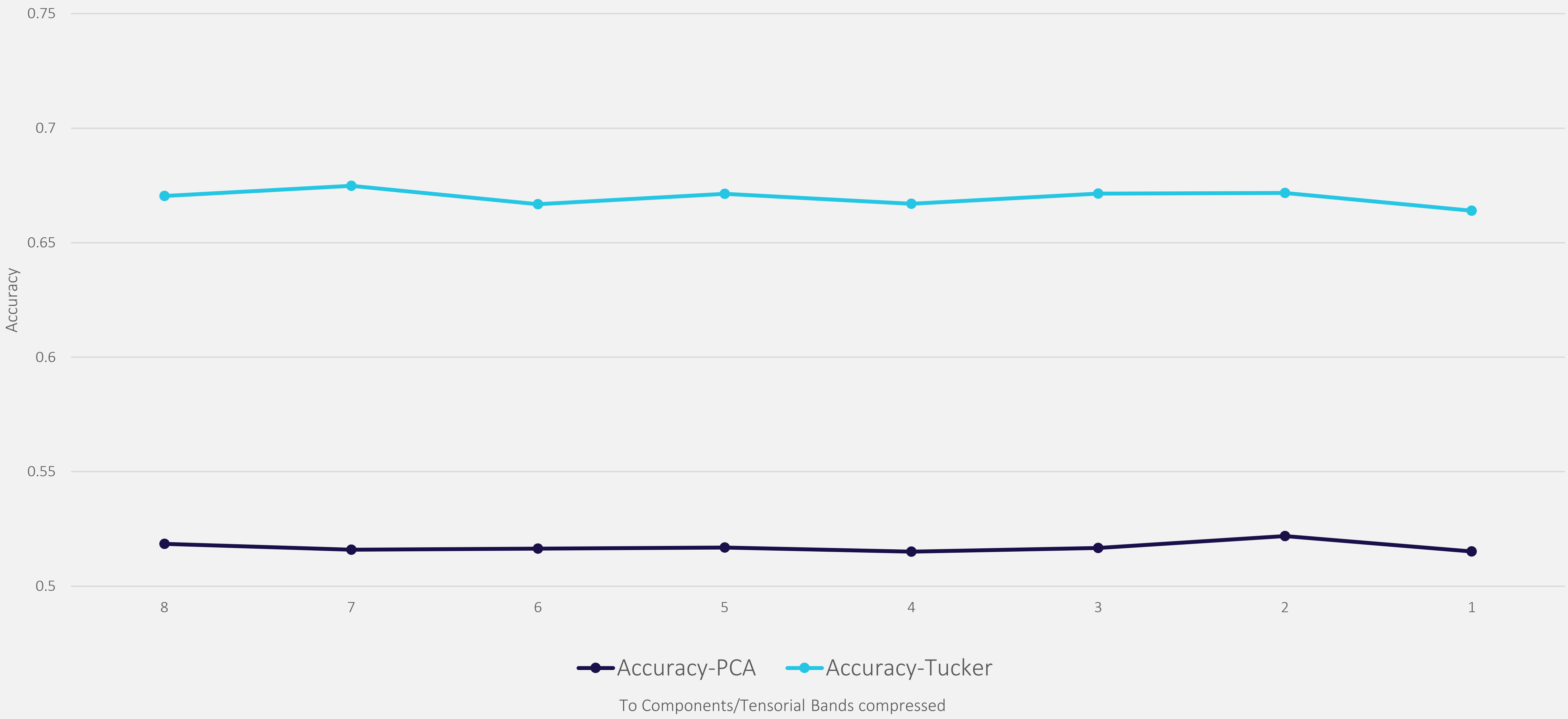

Accuracy Analysis – Noise Added: $\sigma = 82$ and $\eta = 72$

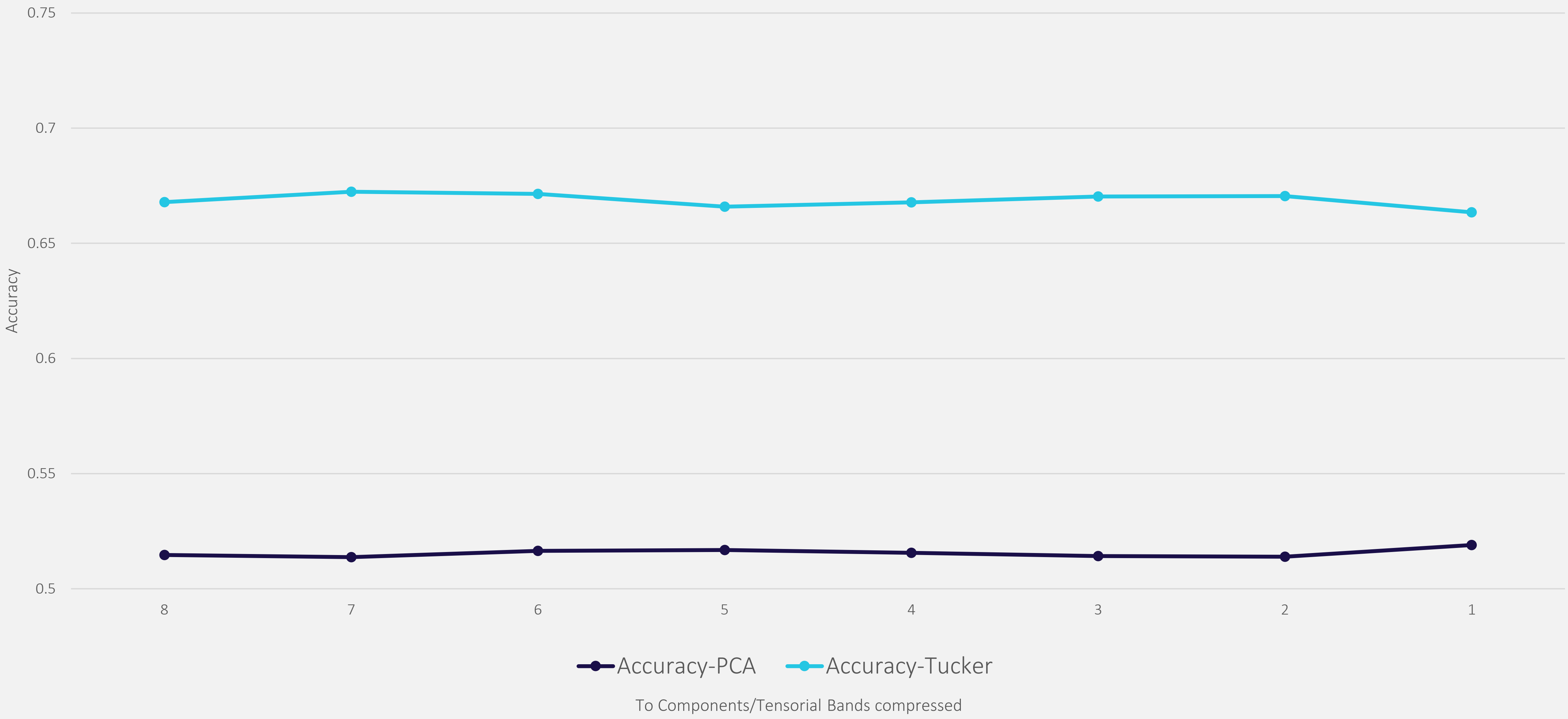

Conclusions

- An experiment was proposed to observe the behavior of the classification accuracy after compression methods.
- We can observe that the accuracy generally increment compressing to 6 or 7 bands instead of 8 with Tucker Decomposition.
- We can attribute that the information in this less significative bands is in its majority noise.
- Lower SNR minimize this phenomenon.
- Tucker Decomposition generally perform better compression than PCA.

Future Work

- To improve the classifier to get higher accuracies and maximize this phenomenology.
- Compare with a noise-free spectral image.

References

[1] M. Borengasser, W. Hungate, and R. Watkins, *Hyperspectral remote sensing: principles and applications*. 2007.

[2] T. G. Kolda and B. W. Bader, “Tensor decompositions and applications,” *SIAM Review*, vol. 51, no. 3. pp. 455–500, 2009.

[3] X. Kong, Y. Zhao, J. Xue, and J. C.-W. Chan, “Hyperspectral Image Denoising Using Global Weighted Tensor Norm Minimum and Nonlocal Low-Rank Approximation,” *Remote Sens.*, vol. 11, no. 19, p. 2281, Sep. 2019, doi: 10.3390/rs11192281.

[4] B. Rasti, P. Scheunders, P. Ghamisi, G. Licciardi, and J. Chanussot, “Noise Reduction in Hyperspectral Imagery: Overview and Application,” *Remote Sens.*, vol. 10, no. 3, p. 482, Mar. 2018, doi: 10.3390/rs10030482.

[5] O. Sidorov and J. Y. Hardeberg, “Deep Hyperspectral Prior: Denoising, Inpainting, Super-Resolution,” Feb. 2019.

[6] N. Acito, M. Diani, and G. Corsini, “Signal-dependent noise modeling and model parameter estimation in hyperspectral images,” *IEEE Trans. Geosci. Remote Sens.*, vol. 49, no. 8, pp. 2957–2971, Aug. 2011.

References

[7] W. Xie and Y. Li, “Hyperspectral Imagery Denoising by Deep Learning with Trainable Nonlinearity Function,” *IEEE Geosci. Remote Sens. Lett.*, vol. 14, no. 11, pp. 1963–1967, Nov. 2017.

[8] C. Wang, L. Zhang, W. Wei, and Y. Zhang, “When Low Rank Representation Based Hyperspectral Imagery Classification Meets Segmented Stacked Denoising Auto-Encoder Based Spatial-Spectral Feature,” *Remote Sens.*, vol. 10, no. 2, p. 284, Feb. 2018.

[9] A. Maffei, J. M. Haut, M. E. Paoletti, J. Plaza, L. Bruzone, and A. Plaza, “Efficient Convolutional Neural Network for Spectral-Spatial Hyperspectral Denoising,” in *Workshop on Hyperspectral Image and Signal Processing, Evolution in Remote Sensing*, 2019, vol. 2019-Septe.

[10] O. Sidorov and J. Y. Hardeberg, “Deep Hyperspectral Prior: Denoising, Inpainting, Super-Resolution,” Feb. 2019.

[11] Q. Yuan, Q. Zhang, J. Li, H. Shen, and L. Zhang, “Hyperspectral image denoising employing a spatial-spectral deep residual convolutional neural network,” *IEEE Trans. Geosci. Remote Sens.*, vol. 57, no. 2, pp. 1205–1218, Feb. 2019.

[12] W. Shan, P. Liu, L. Mu, C. Cao, and G. He, “Hyperspectral Image Denoising With Dual Deep CNN,” *IEEE Access*, vol. 7, pp. 171297–171312, Nov. 2019.

[13] W. Dong, H. Wang, F. Wu, G. Shi, and X. Li, “Deep Spatial–Spectral Representation Learning for Hyperspectral Image Denoising,” *IEEE Trans. Comput. Imaging*, vol. 5, no. 4, pp. 635–648, Apr. 2019.

[14] W. Liu and J. Lee, “A 3-D Atrous Convolution Neural Network for Hyperspectral Image Denoising,” *IEEE Trans. Geosci. Remote Sens.*, vol. 57, no. 8, pp. 5701–5715, Aug. 2019.

[15] Z. Wang, Q. She, and T. E. Ward, “Generative Adversarial Networks in Computer Vision: A Survey and Taxonomy,” Jun. 2019.

[16] J. López, D. Torres, S. Santos, and C. Atzberger, “Spectral Imagery Tensor Decomposition for Semantic Segmentation of Remote Sensing Data through Fully Convolutional Networks,” *Remote Sens.*, vol. 12, no. 3, p. 517, Feb. 2020, doi: 10.3390/rs12030517.

[17] J. M. Bioucas-Dias and J. M. P. Nascimento, “Hyperspectral Subspace Identification,” *IEEE Trans. Geosci. Remote Sens.*, vol. 46, no. 8, 2008, doi: 10.1109/TGRS.2008.918089.

[18] F. Pedregosa *et al.*, “Scikit-learn: Machine learning in Python,” *J. Mach. Learn. Res.*, vol. 12, pp. 2825–2830, Oct. 2011.

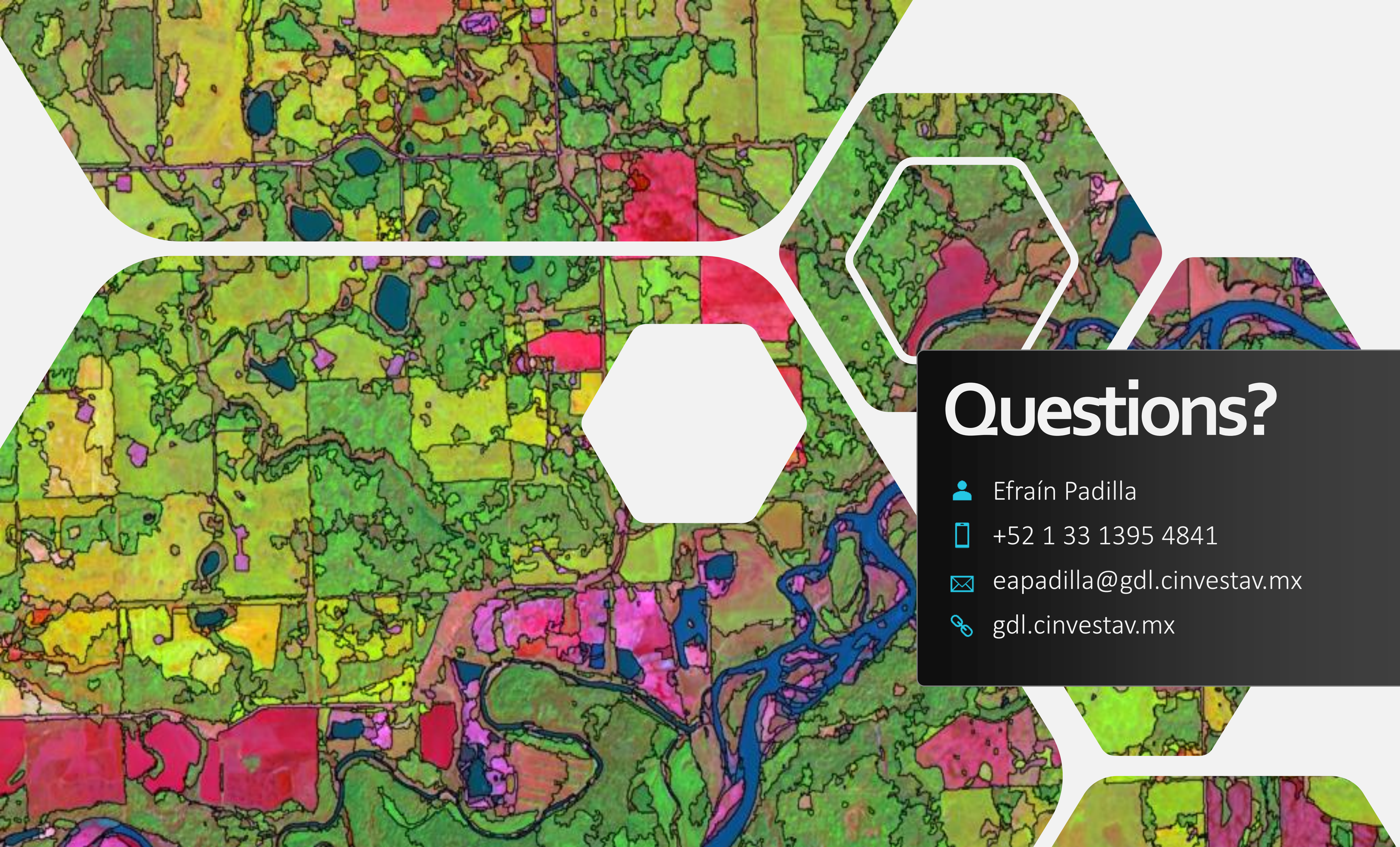

Questions?

Efraín Padilla

+52 1 33 1395 4841

eapadilla@gdl.cinvestav.mx

gdl.cinvestav.mx

Backup

- Signal dependent Noise [4]
  - Shot (photon) noise in HSI is modeled by the Poisson distribution for which the noise variance is signal dependent. The noise variance estimation under this assumption is more challenging than in the signal independent case.

  - The generic Hyperspectral pixel $\mathbf{X}$ can be viewed as an $N_B \times 1$ (N_B being the number of sensor channels) modeled as

$$\mathbf{X} = \mathbf{s} + \mathbf{N}(\mathbf{s})$$

Where $\mathbf{s} = [s_1, ..., s_{N_B}]^T$ is the vector denoting the useful signal in the N_B sensor channels and $\mathbf{N(s)} = [N_1(s_1), ..., N_{N_B}(s_{n_B})]^T$ represents the random noise vector. [6]

Backup - SNR

Evaluate Restoration Results

$$\mathrm{SNR}_{\mathrm{in}} = 10\log_{10}\left(\|\mathbf{X}\|_F^2 / \|\mathbf{X} - \mathbf{H}\|_F^2\right)$$

$$\mathrm{SNR}_{\mathrm{out}} = 10\log_{10}\left(\|\mathbf{X}\|_F^2 / \|\mathbf{X} - \hat{\mathbf{X}}\|_F^2\right)$$

ECORFAN®